THE EFFECTS OF NON-CONDENSABLE GASES ON THE CONDENSATION HEAT TRANSFER OF HFE7100 IN IMMERSION COOLING SYSTEMS

L.-H. Chien[1*, 2] C.-H. Lin[1], C.-W. Hsu[1] and S.-H. Cai[1]

[1]Research Center of Energy Conservation for New Generation of Residential, Commercial, and Industrial Sectors, National Taipei University of Technology, 1, Sec 3, Chung-Hsiao E Rd., Taipei 106, Taiwan

[2]Department of Energy and Refrigerating Air-conditioning, National Taipei University of Technology, 1, Sec 3, Chung-Hsiao E Rd., Taipei 106, Taiwan

* Corresponding Author: lhchien@ntut.edu.tw

Keywords: Immersion cooling, Non-condensable gas, Dielectric fluids, Condensation

ABSTRACT

This study conducted the condensation heat transfer experiment of HFE-7100 with non-condensable gases on the plain tube and fin tube. The saturation temperature of the system was 50°C, the heat flux ranges from 8000 to 18000W/m^2. Four tubes are arranged in a vertical row. The outside diameter of the tubes is 19.05mm and 18.42mm for the plain and fin tubes, respectively. The mass fractions (W_a) of the non-condensable gas varied from 0, 0.5, 1, and 2% in the chamber. The cooling water flows into the tubes from either the top or bottom end, and the tube bundle with two tilting angles, 0°, 30°, were tested. The experimental results showed that the condensation heat transfer of both tube types decreases with the increase of non-condensable gas concentration. The heat transfer coefficient of the fin tube is about 10 times better than the plain tube in pure vapor, but the influence of non-condensable gas is more severe for the fin tube. When W_a is 2%, the heat transfer coefficient of the fin tube decreases by about 80% as compared with pure vapor. The heat transfer ability for cooling water entering from the top is better than that from the bottom, and it is better for a tilting angle 30° than that for 0° with fixing other test parameters.

INTRODUCTION

As the performance of data center servers improves, power consumption also increases. Cooling demand also accounts for about half of the power consumption of data centers. The need to remove the heat energy generated by the computers also increases. Increasing the effectiveness of cooling to improve energy efficiency is an important issue. The two-phase immersion cooling system puts the heating electronic components directly into the dielectric liquids so that the heat is directly transferred into the liquid by boiling the low-boiling-point liquid. During the process, the boiling bubbles will take away heat, while the condensate will flow back to the heating area under the influence of gravity. Neither vapor nor liquid flow requires additional power. Hence, it can significantly reduce energy consumption and provide higher efficiency. Condensation heat transfer is an important element in the immersion cooling system. Beatty and Katz (1) established a prediction formula for condensation heat transfer outside a horizontal low-finned tube. Their prediction model postulated that the gravity, viscosity of the liquid surface, and the influence of the surface tension of the liquid film mainly influence the condensate. Their prediction of the condensation heat transfer coefficient is multiplied by the enhancement ratio of the Nusselt (2) theory.

One of the problems encountered in the practical application of the two-phase immersion cooling system is that there is non-condensable gas in the system. Due to the need to maintain the computational facilities, it is difficult to avoid air entering the system during maintenance. Due to different saturation temperatures, the air will not be condensed but will remain in the system. In addition to causing the vapor partial pressure of the working fluid to decrease, lowering the saturation temperature, and requiring lower condensation surface temperature, the vapor will approach the condenser tube during condensation and gather near the condenser tube, forming an air film, which will reduce the condensation performance. Just a small amount of non-condensable gas can significantly reduce condensing heat transfer performance. This experiment uses the non-conductive fluid HFE-7100 as the working fluid and uses two types of tube arrays, with smooth tubes and fins as the condensation side, to conduct a two-phase condensation experiment with various concentrations of the non-condensable gases. The flooding effect of condensate on the condensation heat transfer performance of a vertical row of tubes is also investigated by changing the angle of the tube array arrangement.

EXPERIMENTAL SETUP

The experimental system is shown in Figure 1. The test chamber is a closed container composed of a stainless shell and two cover plates. An O-ring is placed between the shell and the cover plate to ensure air tightness. The length, width, and height of the cavity are 460, 330, and 50mm, respectively. An array of condensation tubes is placed in the upper half. Cold water flows in the tubes as the condensation side and is connected to a constant-temperature bath to control the temperature. An electric heating tube will be placed in the lower half of the evaporation side. Powered by the power supply, the working fluid will form a closed evaporation and condensation cycle in the cavity. The distance from the center of the uppermost tube of the

condensation tube to the top of the test chamber is 50mm, and the distance from the center of the lower condensation tube to the bottom of the chamber is 130mm. The distance from the center of the electric heating tube to the bottom of the chamber is 45mm. The working fluid filled to a distance of 80mm from the bottom of the chamber. A layer of metal mesh is placed above the liquid interface to prevent splashing. There are two temperature sensors installed in the chamber, one for the upper half and the other in the lower half to confirm whether the evaporation side and the condensation side of the chamber have reached the saturation temperature. There is also a pressure sensor on top of the chamber to confirm the saturation status. The gas temporary storage tank is installed in the upper half of the chamber for charging the non-condensable gas, and is equipped with a pressure sensor to confirm how much non-condensable gas is input into the tank. There is a sight glass window with a diameter of 170mm on the side of the test chamber, and a transparent PC board is installed in the window to observe the condensation phenomena of the tube array.

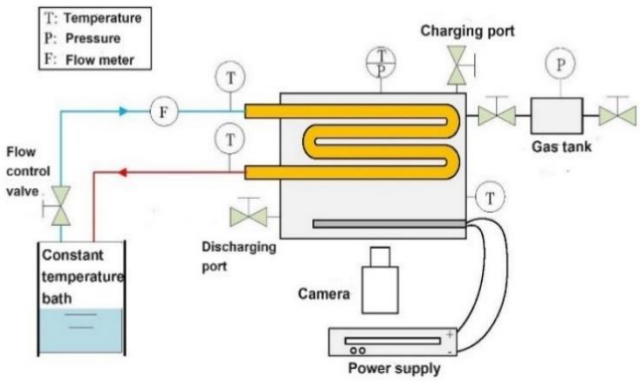

Figure 1. Test apparatus of external condensation with non-condensable gases

Experimental Test Scope

The working fluid, HFE7100 was tested at 72.8 kPa (Tsat ≅50°C) with additional non-condensible gas of 0~2% concentration. The test scope of this study is listed in Table 1. Two types of tubes were tested. Four 380 mm long tubes were connected in the test chamber to form a tube array for each type of tubes. The plain tubes have no fins on both outside and inside. The fin-tubes has external fins of 51 fins/in, 0.6 mm fin height, 0.3 mm fin thickness, and internal spiral fins of 0.22 mm fin height with 38 leads in 42° spiral angle.

Data Reduction

The heat transfer rate (Q) on the waterside can be calculated through the water temperature ($T_{c,\,in}$, $T_{c.out}$) and flow rate at the inlet and outlet of the tube as given in Eq. (1). The heat flux is defined by Eq. (2). Based on energy conservation, the total heat transfer rate (Q) and the heat transfer rate on the water side (Q_w) are equal.

Table 1. Test scope

Working fluid	HFE-7100
Saturation Pressure, P_{sat}	72.8kPa
Non-condensable gas concentration, W_a	0, 0.5%, 1%, 2%
Tube type	Plain tube, Fin-tube
Tube diameters (mm)	Plain: 19.05 OD, 16.85 ID Fin-Tube:18.42OD, 16.05ID
Cooling Rate, Q	680~1421 W
Inclination angle	0°, 30°

The (UA) is then calculated using the logarithmic mean temperature difference (LMTD) method, given by Equation (3) and (4).The condensation heat transfer outside the tube (h_o) can be calculated by subtracting the conduction resistance and the internal convection resistance ($1/h_iA_i$) from the total resistance in Eq. (5)

$$Q = m_w \cdot c_{p,w} \cdot (T_{w,out} - T_{w,in}) \quad (1)$$

$$q" = \frac{Q}{A} \quad (2)$$

$$LMTD = \frac{(T_s - T_{w,in}) - (T_s - T_{w,out})}{ln\left[\frac{(T_s - T_{w,in})}{T_s - T_{w,out}}\right]} \quad (3)$$

$$UA = \frac{Q}{LMTD} \quad (4)$$

$$\frac{1}{UA} = \frac{1}{h_o A_o} + \frac{ln(d_o/d_i)}{2\pi LK} + \frac{1}{h_i A_i} \quad (5)$$

The internal convection heat transfer coefficient of the smooth tube can be calculated through the Gnielinski equation in Eq. (6), where the friction factor f, and Re number are calculated by Eq. (7) and (8). As for the internal finned tube, the internal convection heat transfer coefficient is calculated using the empirical correlation proposed by Ravigururajan and Bergles (3).

$$Nu = \frac{h_i d_i}{k_w} = \frac{\left(\frac{f}{8}\right)(Re_w - 1000)Pr_w}{1 + 12.7\left(\frac{f}{8}\right)^{\frac{1}{2}}\left(Pr_w^{\frac{2}{3}} - 1\right)} \quad (6)$$

$$f = (0.79\, lnRe_w - 1.64)^{-2} \quad (7)$$

$$Re_{d_i} = \frac{\rho_w v d_i}{\mu_w} \quad (8)$$

The modified Wilson plot (4) method is used to correct the tube's heat transfer coefficient based on the tested tubes' experimental data to obtain an accurate heat transfer coefficient outside the tube. From Eq. (5), the overall heat transfer coefficient can be calculated by Eq. (9).

$$\frac{A_o}{UA} = a\frac{1}{h_i} + b \quad (9)$$

The values of a and b are constant if the heat flux remains constant and can be given by Eq. (10) and (11).

$$a = \frac{d_o}{d_i}\frac{1}{c_i} \quad (10)$$

$$b = A_o \frac{\ln(d_o/d_i)}{2\pi Lk} + \frac{1}{h_o} \quad (11)$$

From the regression of the experimental data, the value of c_i , can be found to find the corrected internal convection heat transfer coefficient, given by Eq.(12).

$$h_i^* = c_i \times h_i \tag{12}$$

The mass flux of vapor flow, G, is calculated by Eq. (13), where the mass flow rate is estimated by heat input, and the cross-sectional area is calculated based on the chamber's internal dimensions.

$$G = \frac{m_v}{A} = \frac{Q}{h_{fg}A} \tag{13}$$

Uncertainty Analysis

The uncertainty analysis in this experiment adopts the experimental uncertainty calculation formula as shown in equation (14).

$$\frac{\omega(\mathrm{R})}{\mathrm{R}} = \sqrt{\left(\frac{\partial \mathrm{R}}{\partial \mathrm{x}_1}\cdot\frac{\omega(\mathrm{x}_1)}{\mathrm{R}}\right)^2 + \cdots + \left(\frac{\partial \mathrm{R}}{\partial \mathrm{x}_\mathrm{n}}\cdot\frac{\omega(\mathrm{x}_\mathrm{n})}{\mathrm{R}}\right)^2} \tag{14}$$

The x_n in Eq. (14) is the parameter affected by each item, and the number of influencing parameters varies according to the experiment. The parameters that affect the heat transfer coefficient in this experiment include the heat transfer measured by water and the logarithmic average temperature difference of the double-casing heat exchanger. The measuring instruments used in this experiment, and their accuracy are: (Coriolis) flow meter 0~30 LPM ±0.1%; RTD: ±0.08℃;Thermocouple: ±0.16℃. Bring in the error value of each RTD according to the calibration results. The uncertainty of the condensation heat transfer coefficient under all experimental conditions can be obtained. The uncertainty of the condensation heat transfer coefficient in this experiment is 3.8~7.7% for the plain tubes and 5.1~19.4% for the fin tubes.

RESULTS AND DISCUSSION

Verification with the Nusselt's theory

Figure 2 compares the heat transfer performance of pure steam on the tilted tube array with the cold water entering from the top end and Nusselt's condensation theory (2) of a single horizontal tube. The reason for selecting this data is that each single tube is not affected by the condensation liquid above. The results show that the experimental data falls within 15% of the prediction by the Nusselt' theory.

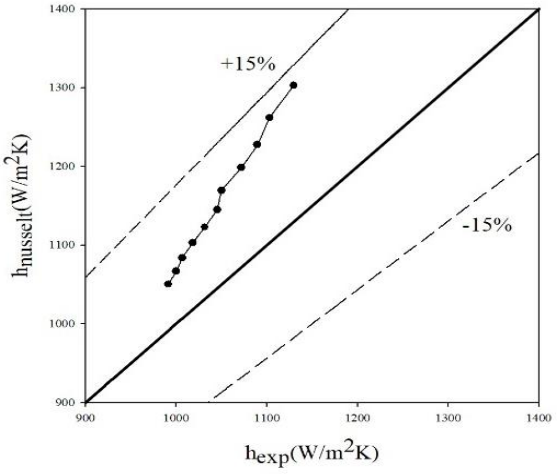

Figure 2. Comparison of the condensation test on the plain tube in the inclined tests with Nusselt's theory

Effect of Non-condensable Gases on Condensation on the Plain Tubes

The impact of pure steam and three non-condensable gas mass concentrations (Wa) of 0%, 0.5%, 1%, and 2% on condensation heat transfer performance of vertically aligned plain tubes are shown in Figures 3 and 4, with the cold water entering from the top end or the bottom end, respectively. As shown In Figure 3, the heat transfer performance gradually increases and then levels off as the heat flux increases. The heat transfer performance is quite close to that of the pure fluid when Wa is 0.5%.

When the mass concentration of the non-condensable (Wa) reaches 1% , the heat transfer performance is affected under low heat flux, which is 8.34% lower than that of pure steam. When Wa reaches 2%, it is most severely affected by non-condensable gas, and the overall condensation heat transfer performance is reduced by 30.9% compared with pure steam. Figure 4 also shows a similar trend when water enters from the bottom ends.

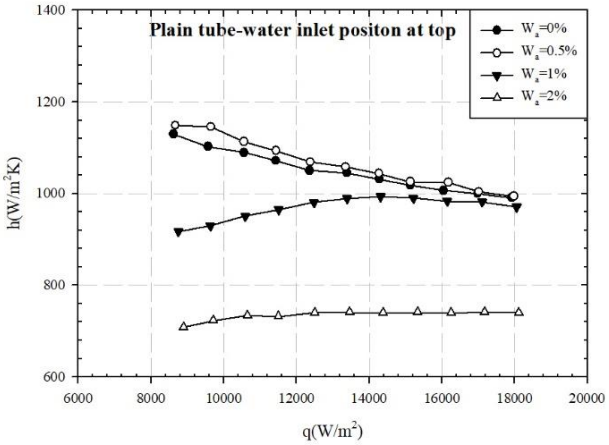

Figure 3. Condensation on the plain tube array with water entering from the top end

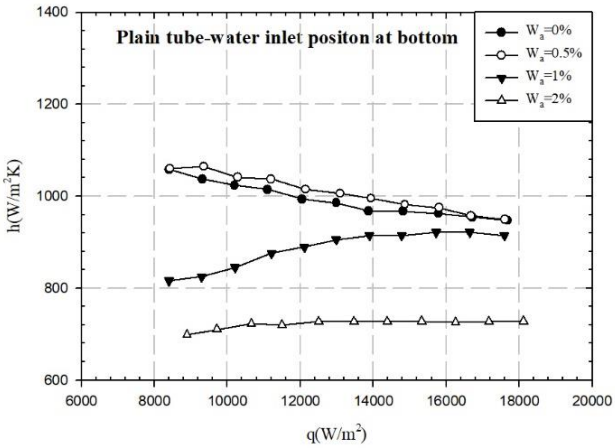

Figure 4. Condensation on the plain tube array with water entering from the bottom end

Condensation on the Plain Tubes in the Inclined Array

The effects of inclination and water inlets are compared in Figures 5 and 6 with the concentrations of non-

condensable gas at Wa = 0%, and 0.5%, respectively. It can be found that in the same cold water inlet direction, the condensation heat transfer coefficient is higher when the array is inclined as compared with that in the non-inclined tests. This is because that the dripping condensation droplets will not fall on the tube below when the array is inclined. The condensation condition of each tube in the inclined array is closer to that of a single tube. Hence, the average liquid film thicker is thinner, resulting in a higher overall condensation heat transfer performance. When the cavity is not inclined, the condensate accumulated on the lower tube is thicker as it received the condensation droplets above, reducing the effective heat transfer area and reducing heat transfer performance. Figure 5 also shows that when the array is inclined, the heat transfer performance of both cold water entry directions is quite close. However, the condensation performance with cold water entering from the top is better than that from the bottom in the non-inclined tests. This indicates that the effective area in the lower tube is smaller because of the influence of condensation droplets in the inclined tests. When cold water enters from the bottom, the temperature difference between the hot and cold fluid is larger but heat exchange is not effective because the effective area and the condensation heat transfer coefficient are smaller at the lower tubes. Similarly, the condensation heat transfer coefficients for the inclined tests are higher than those in non-inclined tests, and water entering from the top results in greater condensation performance for W_a = 0.5% in Figure 6. Figure 7 shows the similar effects on inclination with the concentrations of non-condensable gas at W_a = 2%. However, the heat transfer coefficient with water entering from bottom in the inclined tests shows more significant degradation at W_a = 2.0%, and yields the lowest heat transfer coefficient, which is even smaller than that in the non-inclined tests.

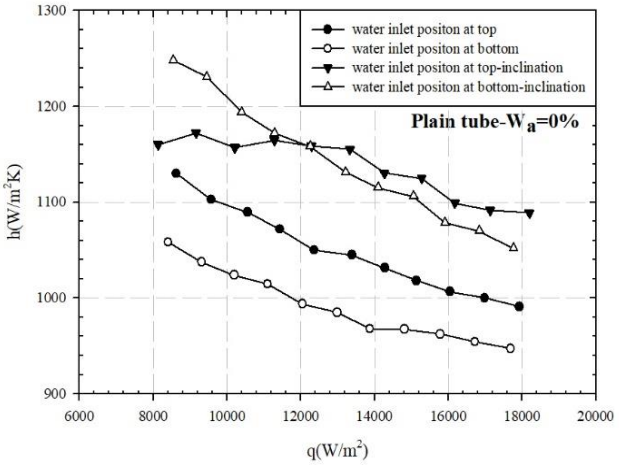

Figure 5. Effect of inclination on Condensation of the plain tube with different water inlets at W_a = 0%

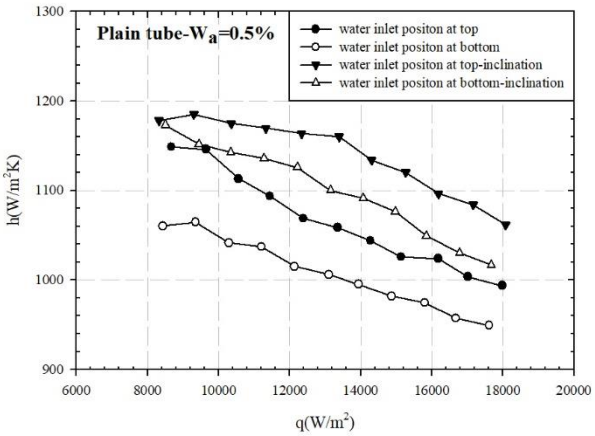

Figure 6. Effect of inclination on Condensation of the plain tube with different water inlets at W_a = 0.5 %

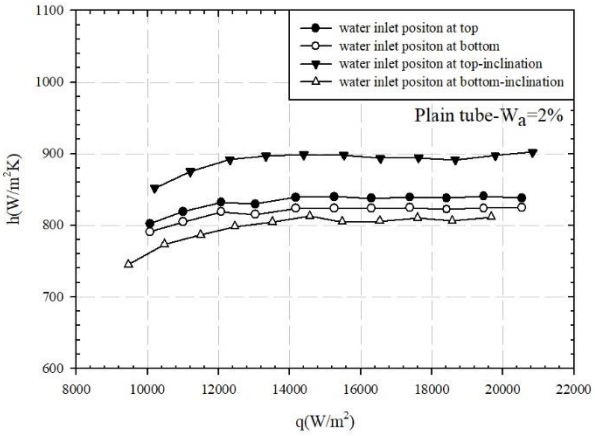

Figure 7. Effect of inclination on Condensation of the plain tube with different water inlets at W_a = 2.0 %

Condensation on the Fin-tube

Figure 8 shows the condensation heat transfer coefficient outside the tube with the heat flux under different non-condensable gas concentrations in the non-inclined tests with the cold water entering from the top end. Without non-condensable gas, the heat transfer coefficient varied between 9,000 to 11,000 W/m^{2}K, which is about 9 to 10 folds of that of the plain tube. When W_a reaches 0.5%, the heat transfer performance is significantly lower than that of pure steam, and the heat transfer performance drops by 34.4%. When W_a reaches 1%, the heat transfer performance continues to be reduced by the influence of non-condensable gas, which is 57.9% lower than that of pure vapor. When W_a reaches 2%, the heat transfer performance is the worst, which is 80.5% lower than that of pure vapor.

Figure 9 compares the experimental data of fin tubes in pure vapor with the empirical formula of low-fin tubes by Beatty and Katz (1). The fin used in this experiment has a tiny jagged structure. In order to simplify the calculation process, the influence of the surface structure is ignored in the prediction. From Figure 13, we found that most of the experimental data fall within the range of +30%. The correlation of Ross (5) for condensation on low-fin tubes has also been compared with the present

data with 20~40% underprediction. The underestimation could result from the ignored surface tension effect on the jagged structure in the present fin tubes.

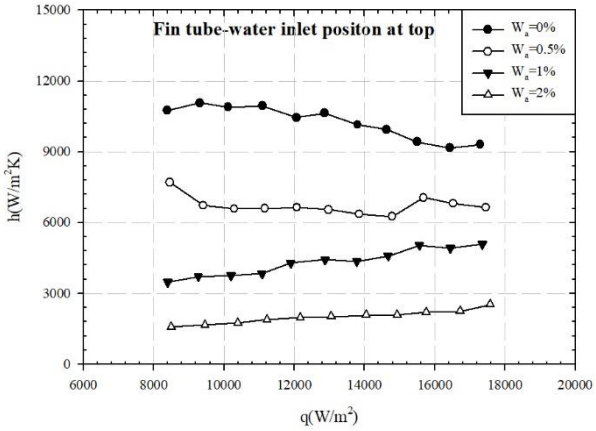

Figure 8. Condensation on the fin-tube array with water entering from the top end

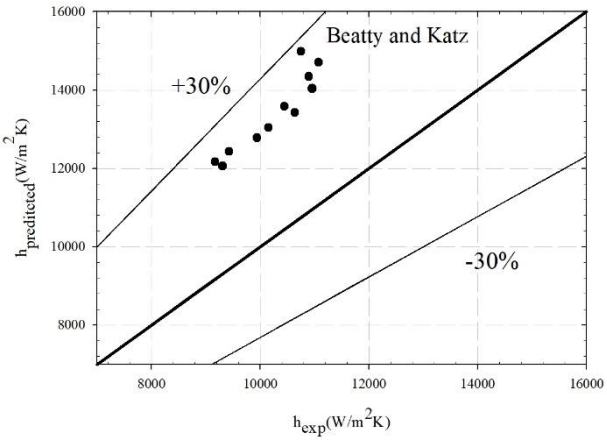

Figure 9. Comparison of the condensation on the fin-tube in the inclined tests with the Beatty and Katz [5] correlation

Comparison of the Present Test with the Literature

Comparison of the present experimental data of fin tubes and plain tubes with the experimental data of Liu (6) et al. are shown in Figures 10 and 11. Their experimental conditions are the saturation temperature of PF-5060 at a saturation pressure of 70kPa, that is, when the non-condensable gas is in the system, the partial pressure of vapor is still 70kPa. Their condensation section also consists of four condensation tubes forming a tube array. Cold water enters from the top. The working fluid vapor is transported outside the test vessel from a connected pipe by a pump. The fin tubes chosen for comparison with this experiment are in a zigzag shape, similar to the fin shape in this experiment. From Figure 10 and 11, it is found that when there is no non-condensable gas, the condensation heat transfer performance is quite close. When the concentration of non-condensable gas is high, the fin heat transfer performance of the two working liquids is also greatly affected. In Figure 10, the heat transfer performances show a decreasing trend with the increase of heat flux, while in Figure 11, the heat transfer performance of the fin tube in HFE-7100 is greater than that of the Jagged fin tube in Liu (6) et al; it increases with the increase of temperature difference.

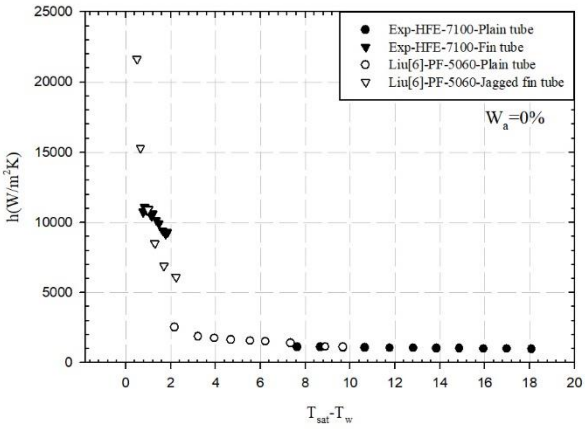

Figure 10. Comparison of condensation test results with Liu (6) et al. without non-condensable gas

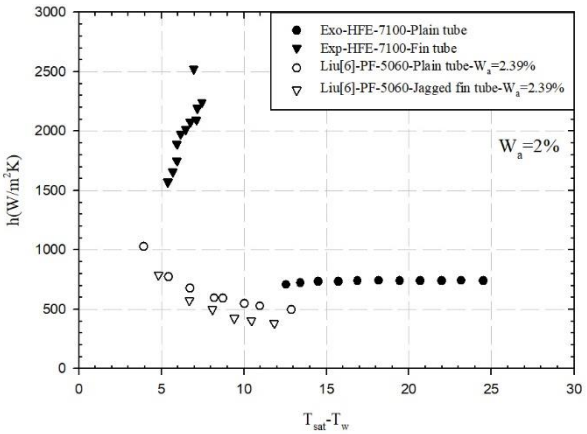

Figure 11. Comparison of condensation test results with Liu (6) et al. with 2% non-condensable gas

CONCLUSIONS

From the present tests of condensation in HFE 7100, we conclude:

1. The condensation heat transfer performance of the plain tube is insignificantly influence by the non-condensable gas when the concentration W_a is 0.5%. When W_a is 1%, it is 8.34% lower than that of pure vapor. Significant reduction on condensation performance is observed when W_a is 2%, and the decrease in heat transfer coefficient is 30.9%.
2. The condensation heat transfer performance of fins is better than that of the plain tubes, which is 9.77 times. However, it is also more seriously affected by non-condensable gases. When W_a is 0.5%, the heat transfer performance is similar to that of pure vapor. When Wa is 1%, it is 57.9% lower than that of pure vapor. When Wa reaches 2%, it is reduced by 80.5%.
3. When the test section is inclined, the condensation tube is not affected by dripping liquid, and the condensation heat transfer performance is better than

that in the non-inclined tests.

4. Different cold water entry configurations will affect the overall condensation performance. When cold water enters from the bottom, the condensation heat transfer performance will be worse than from the top end. This is because the liquid film increases in the condensation tube below. Thick liquid film seriously hinders heat exchange on the lower tubes.

ACKNOWLEDGMENT

This paper represents the research project's outcomes funded by the National Science Council under project number NSTC 110-2221-E-027 -062 -MY2 and the Higher Education Sprout Project, Research Center of New Generation Energy Conservation, from the Ministry of Education.

NOMENCLATURE

c_p	specific heat	J/(kg · K)
d	tube diameter	mm
f	friction factor	-
h	heat transfer coefficient	W/(m^2 · K)
k	conductivity	W/(m · K)
LMTD	log mean temperature difference	ºC
m	mass flow rate	kg/s
Nu	Nusselt number	-
P	pressure	kPa
Re	Reynolds number	-
Q	heat transfer rate	W
T	temperature	ºC
U	overall heat transfer coefficient	W/(m^2 · K)
W_a	non-condensable gas concentration	%
ρ	density	kg/m^3

Subscripts

a	non-condensable gas
i	internal
sat	saturated
o	external

REFERENCES

(1) Beatty, K.O. and Katz. D.L. (1948): “Condensation of Vapors on Outside of Finned Tubes”. *Chemical Engineering Progress*, Vol. 44, pp. 55-70.

(2) Nusselt W.(1916): “Die oberflachenkondensation des wasserdampfes”. *VDI-Z (Ver Dtsch Ingenieure-Z)*, Vol. 60, No. 28, pp. 569-575.

(3) Ravigururajan, T.S. and Bergles, A.E.(1996): “Development and verification of general correlations for pressure drop and heat transfer in single-phase turbulent flow in enhanced tubes”. *Experimental Thermal and Fluid Science*, Vol. 13, pp. 55-70.

(4) Briggs, D.E. and Young, E.H.(1969): “Modified Wilson plot techniques for obtaining heat transfer correlations for shell and tube heat exchangers”. *Chemical Engineering Progress Symposium Series* Vol. 92, No. 65 , pp. 35-45.

(5) Rose, J.W.(1994): “An approximate equation for the vapour-side heat-transfer coefficient for condensation on low-finned tubes”. *Int. J. Heat Mass Transfer*, Vol. 37, pp. 865-875.

(6) Liu, P., Kandasamy, R., Ho, J. Y., & Wong, T. N. (2020): “An experimental investigation on the effects of air on filmwise condensation of PF-5060 dielectric fluid on plain and finned tube bundles”. *Int. J. Heat Mass Transfer*, Vol.162 , Article 120349.